

VU Research Portal

Comparative study of spectral flexibilities of bacterial light-harvesting complexes: Structural implications

Rutkauskas, D.; Olsen, J.; Gall, A.; Cogdell, R.J.; Hunter, C.N.; van Grondelle, R.

published in

Biophysical Journal
2006

DOI (link to publisher)

[10.1529/biophysj.105.075895](https://doi.org/10.1529/biophysj.105.075895)

document version

Publisher's PDF, also known as Version of record

[Link to publication in VU Research Portal](#)

citation for published version (APA)

Rutkauskas, D., Olsen, J., Gall, A., Cogdell, R. J., Hunter, C. N., & van Grondelle, R. (2006). Comparative study of spectral flexibilities of bacterial light-harvesting complexes: Structural implications. *Biophysical Journal*, 90(7), 2463-2474. <https://doi.org/10.1529/biophysj.105.075895>

General rights

Copyright and moral rights for the publications made accessible in the public portal are retained by the authors and/or other copyright owners and it is a condition of accessing publications that users recognise and abide by the legal requirements associated with these rights.

- Users may download and print one copy of any publication from the public portal for the purpose of private study or research.
- You may not further distribute the material or use it for any profit-making activity or commercial gain
- You may freely distribute the URL identifying the publication in the public portal ?

Take down policy

If you believe that this document breaches copyright please contact us providing details, and we will remove access to the work immediately and investigate your claim.

E-mail address:

vuresearchportal.ub@vu.nl

Comparative Study of Spectral Flexibilities of Bacterial Light-Harvesting Complexes: Structural Implications

Danielis Rutkauskas,* John Olsen,[†] Andrew Gall,[‡] Richard J. Cogdell,[‡] C. Neil Hunter,[†] and Rienk van Grondelle*

*Department of Biophysics and Physics of Complex Systems, Division of Physics and Astronomy, Faculty of Sciences, Vrije Universiteit, 1081 HV Amsterdam, The Netherlands; [†]Robert Hill Institute for Photosynthesis, Krebs Institute for Biomolecular Research and Department of Molecular Biology and Biotechnology, University of Sheffield, Sheffield S10 2TN, United Kingdom; and [‡]Division of Biochemistry and Molecular Biology, University of Glasgow, Glasgow G12 8QQ, United Kingdom

ABSTRACT This work presents a comparative study of the frequencies of spectral jumping of individual light-harvesting complexes of six different types: LH2 of *Rhodopseudomonas acidophila*, *Rhodobacter sphaeroides*, and *Rhodospirillum molischianum*; LH1 of *Rhodobacter sphaeroides*; and two “domain swap mutants” of LH2 of *Rhodobacter sphaeroides*: PACLH1 and PACLH2mol, in which the α -polypeptide C-terminus is exchanged with the corresponding sequence from LH1 of *Rhodobacter sphaeroides* or LH2 of *Rhodospirillum molischianum*, respectively. The quasistable states of fluorescence peak wavelength that were previously observed for the LH2 of *Rps. acidophila* were confirmed for other species. We also observed occurrences of extremely blue-shifted spectra, which were associated with reversible bleaching of one of the chromophore rings. Different jumping behavior is observed for single complexes of different types investigated with the same equivalent excitation intensity. The differences in spectral diffusion are associated with subtle differences of the binding pocket of B850 pigments and the structural flexibility of the different types of complexes.

INTRODUCTION

In photosynthesis, bacterial light-harvesting pigment-protein complexes capture solar light, thereby initiating a complicated chain of reactions leading to the conservation of energy in the form of stable chemical potential (1). The discovery of high-resolution crystallographic structures of two peripheral light-harvesting complexes (LHCs) of type 2 (LH2) from the purple bacteria *Rhodopseudomonas (Rps.) acidophila* and *Rhodospirillum (Rs.) molischianum* (2–4) has put the previously available biochemical and physical information into a proper structural perspective and, consequently, has resulted in a better physical understanding of the photosynthetic light-harvesting mechanism (5–8) (V. Novoderezhkin and R. van Grondelle, unpublished). The LH2 of *Rps. acidophila* is a highly symmetric ring of nine protein-pigment subunits, each containing two α -helical transmembrane polypeptides: the α -polypeptide on the inner and the β -polypeptide on the outer side of the ring. Close to the C-terminal end of these transmembrane helices a highly conserved His residue forms a ligand to a bacteriochlorophyll *a* (BChl *a*) molecule, resulting in a ring of 18 tightly coupled BChls *a* with a center-to-center distances of slightly <1 nm between neighboring pigments. This ring is responsible for the intense absorption of LH2 at ~850 nm (B850 ring). A second ring of nine weakly interacting BChls *a* is located closer to the N-terminus of the polypeptides and is largely responsible for the absorption at ~800 nm (B800 ring). The LH2 of *Rs.*

molischianum exhibits a similar structure overall with two pigment rings in a protein scaffold similar to that of LH2 of *Rps. acidophila*, but it has eightfold symmetry and a somewhat different pigment arrangement, particularly with respect to the B800 BChls *a*. Although there are no crystal structures of either LH2 or LH1 of *Rhodobacter (Rb.) sphaeroides*, an accurate model of a monomeric LH1 of *Rb. sphaeroides* (without PufX) has been constructed (9) based upon the NMR structure of the β -polypeptide (10), the low-resolution projection map of LH1 of *Rs. rubrum* (5,11), and the structure of the LH2 of *Rs. molischianum*, which shares many protein motifs in common with LH1. The homology of the LH2 of *Rb. sphaeroides* to that of *Rps. acidophila* in light of the cryo-electron microscopy structural information (12) allowed us to use the atomic structure of the latter to model the interactions of the polypeptides with the BChl *a* pigments.

Abundant theoretical and experimental effort has resulted in a detailed model of electronic and energy transfer properties of LHCs (13–19). The two basic features of this model are the excitonic coupling between pigments and the static disorder of the pigment electronic transition energies. Energetic disorder arises from the fact that a protein is intrinsically a disordered system occurring in a number of conformational substates. As a consequence, the electronic transition energies of the different sites are not identical due to the interaction of each chromophore with the surrounding protein.

At physiological and even at cryogenic temperatures a protein is not a rigid entity; it moves in its conformational landscape probing different substates. This was observed in low temperature single-molecule experiments on LH2, where the spectral diffusion of the B800 band was attributed to

Submitted October 12, 2005, and accepted for publication December 16, 2005.

Address reprint requests to Danielis Rutkauskas, Fax: 31-20-5987999; E-mail: danielis@nat.vu.nl.

© 2006 by the Biophysical Society

0006-3495/06/04/2463/12 \$2.00

doi: 10.1529/biophysj.105.075895

structural alterations (20). In later work, spectral fluctuations of varying magnitude occurring on different timescales were associated with the hierarchical structure of protein conformational landscape (21). We have observed changes of the realization of energetic disorder in single-molecule fluorescence (FL) experiments on LH2 of *Rps. acidophila* manifested by spectral changes on the timescale of a second. Calculations, based on the disordered exciton model using the modified Redfield theory to describe exciton relaxation, related these changes to conformational changes of the pigment-protein on a phenomenological level without considering the underlying microscopic detail (22).

Although such an analysis adequately describes the electronic changes of the system, the related microscopic structural alterations are also of interest. It has been suggested that for some proteins, for example, myoglobin (23), conformational changes may be functionally important. The functional role of structural changes in LH2 is open to speculation at this time; one possibility is that the photosynthetic system must be dynamically reorganized in a densely crowded membrane to maintain close ring-to-ring contact. In this work we investigate the possible structural changes by monitoring the FL spectral evolution of individual complexes. The microscopic parameters of protein-pigment interaction, such as hydrogen bonding (H-bonding) between chromophores and the protein, allow us to establish a connection between the observable spectral and structural changes.

Although a large part of the red shift of the B850 ring absorption relative to that of a monomeric BChl *a* is due to excitonic interaction between neighboring BChls *a*, it has been demonstrated that an almost equally significant contribution to this spectral shift originates from protein-pigment interactions (7,24). Even in the absence of precise structural information, evidence of the role of the protein in chromophore absorption was suggested by comparison of polypeptide sequences of LH2 from different species (25). In LH2s absorbing at 850 nm, the primary sequence of the α -polypeptide contains a recurring motif of either Tyr-Trp or Tyr-Tyr residues at positions 43 and 44 (or +13 and +14 counting from the conserved His residue). In a natural variant of LH2 of *Rps. acidophila* absorbing at 820 nm, these two residues are Phe-Leu, whereas the rest of the sequence is very similar. This implied that these conserved residues might be spectroscopically significant. Replacement of either α Tyr+13 or α Tyr+14 with Phe and Leu, respectively, in the LH2 of *Rb. sphaeroides* caused a progressive blue-shifting of the absorption (26,27), and this was associated with the disruption of H-bonds to acetyl carbonyl groups of the B850 BChls *a*. Similar factors were found for the other species based on sequence homology (25) and available structures and models (3,4,28). Summarizing, the following residues form H-bonds to acetyl carbonyl groups of BChls *a* in the B850 (or B870 in case of LH1) ring: LH2 *Rps. acidophila* α Tyr+13(43) and α Trp+14(44), LH2 *Rb. sphaeroides* α Tyr+13(44) and α Tyr+14(45), LH2 *Rs. molischianum*

α Trp+11(45) and β Trp+9(44), and LH1 of *Rb. sphaeroides* α Trp+11(43) and β Trp+9(48). It is noteworthy that in the LH2 of *Rps. acidophila* and *Rb. sphaeroides*, the α -polypeptide donates one H-bond to the acetyl carbonyl of BChl *a* in the same dimeric subunit and a second one to the BChl *a* in the adjacent subunit whereas in the LH2 *Rs. molischianum* and LH1 of *Rb. sphaeroides* both H-bonds are intrasubunit.

Other factors of the pigment interaction with its protein environment that might have an impact on the pigment site energy are the rotation of the acetyl group from the molecular plane (29,30), a deformation of the porphyrin ring (29), its close proximity to point charges (30,31), and the ligation state of the central Mg^{2+} ion (30).

The aforementioned protein-pigment interaction modes connect the microscopic structural detail to the electronic and associated spectroscopic properties of the complex. Changes of these interactions caused by structural fluctuations are associated with the observed temporal evolution of the FL spectrum. Here we study jumps in the emission spectrum upon continuous illumination for different kinds of LHCs. The investigated proteins exhibit a high sequence homology in general but also subtle differences in their B850 pigment binding pocket. We discuss the observed variation of the frequency and size of spectral jumps (spectral flexibility) with the reference to structural diversity of the complexes.

MATERIALS AND METHODS

LH2 complexes of *Rps. acidophila* 10050 and *Rs. molischianum* DSM120 were grown anaerobically at 30°C in Pfennig's medium (32) and modified *Rhodospirillaceae* medium (33), respectively. Cells were harvested by centrifugation. After rupturing the cells in a French press, photosynthetic membranes were obtained by centrifugation. The membranes were solubilized using *N,N*-dimethyldodecylamine-*N*-oxide (LDAO), and the LH2 proteins were purified as described previously (34).

LH2 complexes of *Rb. sphaeroides* and domain swap mutants PACLH1 and PACLH2mol were purified as in Olsen et al. (34) in the DD13 deletion strain.

LH1 membranes were purified according to Olsen et al. (35). The membranes were diluted with a buffer of 1 mM Tris (pH 7.5) and 1 mM EDTA to <5% of sucrose by volume and concentrated by centrifugation for 4 h at 40 krpm in a Beckman (Beckman Coulter, High Wycombe, UK) Ti 45 rotor. The membrane pellet was resuspended in ~1 ml of buffer of 20 mM HEPES (pH 8); ~500 optical density (OD) units of resuspended membranes with OD_{max} at 875 nm were solubilized with 4% *n*-dodecyl- β -D-maltoside (β -DDM), in buffer of 20 mM HEPES (pH 8) and 5 M NaCl solution added to a final concentration of 155 mM NaCl in 10 ml total volume. The β -DDM was added drip-wise to the resuspended membranes with gentle stirring and left to solubilize for 30 min with stirring at 4°C. The solubilized membranes were centrifuged at 48 krpm for 1 h in a Beckman Ti70.1 rotor to remove any unsolubilized material. The solubilized membranes were then loaded onto a DEAE Sepharose column, 15 ml bed volume, preequilibrated with a solution of 155 mM NaCl, 20 mM HEPES (pH 8), and 0.03% β -DDM, and washed for 90 min at 155 mM NaCl concentration and then at 170 mM NaCl for a further 90 min. The purified complexes were then eluted using a 170–400 mM NaCl salt gradient over 60 min and 4 ml fractions collected for analysis. The purest fractions, as ascertained by the 875:280 nm absorbance ratio, were used in a final purification step on a Superose 200 (GE Healthcare Amersham, Chalfont St. Giles, UK) size exclusion column preequilibrated to 155 mM

NaCl, 20 mM HEPES (pH 8), and 0.03% β -DDM. The fraction at the peak of the elution profile was used for a single-molecule spectroscopy.

Stock solutions of all samples were divided into small aliquots and kept at -80°C until thawed and were used only once, thus avoiding repetitive freezing and thawing. For the actual measurement the samples of LH2 of *Rps. acidophila*, *Rb. sphaeroides*, and *Rs. molischianum* were diluted with the buffer of 20 mM Tris (pH 8.0) and 0.1% LDAO. The mutants and LH1 of *Rb. sphaeroides* were diluted in a buffer containing 1% of *n*-octyl- β -D-glucopyranoside (β -OG) without buffer exchange. All the samples were flushed and kept in the deoxygenated buffer, the same as the one used for dilution. The oxygen in the buffers used for flushing was removed by means of a three component oxygen scavenger: 100 \times concentrated water stock solutions containing 20 mg/ml of glucose oxidase and 3.5 mg/ml of catalase were kept at -80°C before use. For deoxygenation 1 ml of stock solution of each component together with 750 mg of glucose were added to 40 ml of buffer, thus fully removing dissolved oxygen. Deoxygenated buffer was kept under N_2 atmosphere before flushing. All the measurements were conducted at 5°C to prolong the survival time of less stable species.

Isolated LH2 and LH1 complexes were immobilized on a standard microscope coverslip covered with poly-L-lysine and submerged in a physiological buffer as described previously (36). Since the pigment-protein complex is effectively immobilized on a monolayer of flexible amino residues, we expect this procedure to be less perturbing than the conventionally used mica or spincoating in a polyvinyl matrix. The confocal setup utilized to acquire sequences of single-molecule FL spectra was based on a commercial biological microscope described earlier (22). This setup has the option of 594 nm excitation with a constant power and random polarization He-Ne laser (Melles Griot (Didam, The Netherlands), 05SYR810-230). With this wavelength, the LHCs were excited in their Q_x absorption band, allowing the use of the long-pass glass filter RG715 (Edmund Optics (York, UK), 46065) with transmission extended further to the blue as compared to the previously utilized broadband interference filter for 800 nm excitation. The effect of the objective achromatism on the excitation and signal collection efficiency was compensated for by decollimating the 594 nm beam before the objective.

Each spectrum in the measured spectral time series was fitted with the skewed Gaussian function to obtain the time dependence of the peak wavelength as was described previously (22).

In earlier work (22,36), we obtained FL time series of spectra for LH2 of *Rps. acidophila* with different excitation intensities at 800 nm. A significant fraction of the complexes evolved between distinctly different and relatively constant quasistable levels of the spectral FL peak wavelength (FLP), and the frequency and size of spectral jumps increased with the excitation intensity. We also assessed the changes of the FL spectral line shape associated with these spectral jumps.

RESULTS

The goal of this work is to compare the spectral flexibilities for a set of different species and to associate the observed differences with variations in the molecular structure. To do so we need consistent data sets: different species were measured at the same temperature of 5°C , upon 594 nm excitation, using a level of absorbed energy equivalent to 2 μW of 800 nm excitation for LH2 of *Rps. acidophila*, which is an intermediate level of excitation intensity compared with the range we probed previously (22,36). Higher excitation intensities at 594 nm were not feasible due to the increased FL background (see below). The corresponding intensities were calculated from the known absorption extinction coefficients (13,37) and the bulk absorption spectra. The following LHCs were investigated: LH2 of *Rps. acidophila*,

Rb. sphaeroides, *Rs. molischianum*, and LH1 of *Rb. sphaeroides*. We obtained 240 spectra for ~ 200 molecules of each species. Exciting at 594 nm instead of 800 nm allowed for the extension of the detection to the blue, since a more blue-shifted emission long-pass filter could be used. In particular this helped the investigation of the changes of the FL profile shape (D. Rutkauskas, V. Novoderezhkin, A. Gall, J. Olsen, R. J. Cogdell, C. N. Hunter, and R. van Grondelle, unpublished). Furthermore, the use of 594 nm excitation enabled us to detect the occurrence of extreme blue spectral jumping and to draw conclusions as to which species are capable of undergoing such drastic transformation.

A second data set with 800 nm excitation was obtained to verify the reproducibility of the relative extent of spectral jumping between different species. The excitation intensity for each type of LHC was again adjusted from the known absorption extinction coefficients and the bulk absorption spectra to be equivalent to 2 μW of 800 nm for LH2 of *Rps. acidophila*. The difference in the size of the focal area for the two wavelengths was not taken into account. Thus, a direct comparison of the two data sets must be done with caution, although the relation between different species within a single data set can in principle be compared with that for a different excitation wavelength. In addition to the four species for which we obtained spectral traces at 594 nm excitation, we measured the domain swap mutants of *Rb. sphaeroides* LH2—PACLH1 and PACLH2mol using only 800 nm excitation light. These mutants have the C-terminal part of the α -polypeptide altered from that of the wild-type (WT) to the same sequence of LH1 of *Rb. sphaeroides* and LH2 of *Rs. molischianum*, respectively (34), which has impaired the FL efficiency. It was not possible to investigate these mutants with 594 nm excitation, since at this wavelength there was significant background FL originating from the glass coverslip in the spectral region of interest, which could not be removed by filtering. For the systems other than these mutants, the signal/noise ratio was sufficient to analyze the FL images and obtain the coordinates of single particles, whereas the FL spectra were corrected by subtracting the background spectrum measured on an area of the coverslip free of fluorescent complexes. However, for 800 nm excitation the background is virtually limited to the dark current of the avalanche photo diode (APD) and the readout noise of a charge-coupled device (CCD) camera allowing the accumulation of data also from species with a relatively low FL efficiency.

Quasistable FLP levels for different species

Recently we made a rather surprising observation that the FLP of a single LH2 of *Rps. acidophila*, of a significant fraction of the complexes measured, evolved through a number of quasistable levels (22,36). This led us to question whether this behavior is characteristic for this particular species or if it is a property of pigment-protein complexes in general. To distinguish such quasistable levels we relied on a

qualitative visual assessment that the variation of the averages of such levels was significantly larger than the fluctuations within the levels. Although less pronounced as in the LH2 of *Rps. acidophila* the spectra of the other species also showed quasistable levels of FLP, which often interchanged without intervening nonradiative periods: examples of spectral traces are shown in Fig. 1. Depending on the excitation wavelength (594 or 800 nm) for LH2 of *Rps. acidophila* between 3% and 10%, respectively, of the measured complexes exhibited quasistable levels of FLP. The corresponding figure for LH2 of *Rb. sphaeroides* was found to be $\sim 11\%$. The domain swap mutant of LH2 of *Rb. sphaeroides*, PACLH1, featured quasistable behavior in 9% of the cases, whereas for PACLH2mol this was $\sim 8\%$. It is also noteworthy that for the two domain swap mutants the spectral shift that occurred most was to an FLP at ~ 880 – 890 nm. This red-shifted level appeared to be very stable, as once in this state most of the complexes remained there until the end of the trace. This does not imply that spectral changes only occurred to the red, but for these mutants we were not able to observe spectral jumps to the blue. This was a consequence of using 800 nm excitation and the FL barrier filter which effectively eliminated jumps to the blue from the average position which is already blue-shifted relative to the WT (FLP distributions for both mutants peak at ~ 845 nm). The LH2 of *Rs. molischianum* and the LH1 of *Rb. sphaeroides* exhibited much less evidence of such quasistable levels: 0.5–1.7% and 0–6%, respectively, for the different data sets with two different excitation wavelengths.

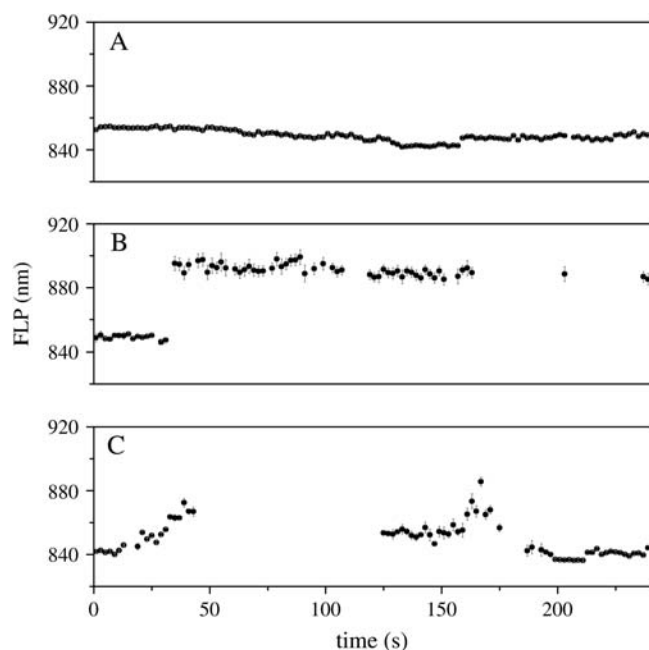


FIGURE 1 Characteristic FLP time traces of three different species of LH2 complexes: (A) *Rb. sphaeroides*, (B) PACLH2mol, and (C) PACLH1. Only every third data point is shown, to improve clarity.

Extreme blue jumps

Excitation at 594 nm instead of 800 nm allowed us to observe extreme blue spectra that were already apparent from the experiment with 800 nm excitation, but could not be visualized to their fullest extent because of the FL filter. It appeared that $\sim 10\%$ of the measured complexes of LH2 of *Rps. acidophila* and *Rb. sphaeroides* (but not *Rs. molischianum*) exhibited transitions to states with spectra peaking at ~ 810 nm and with the full width at half-maximum (~ 20 nm) half of that of the average. An example of such a spectral evolution is shown in Figs. 2 and 3. The peak wavelength of the initial spectrum is ~ 870 nm; in the course of time the spectrum decreases in intensity and broadens and its peak wavelength shifts to the blue. Before the spectrum finally narrows down and settles to an emission maximum at ~ 810 nm, it moves through a state that appears to be a superposition of two fluorescent species with different spectral maxima. Obviously, such a two-component spectrum cannot be satisfactorily fit with the skewed Gaussian function and therefore the corresponding value of the FLP in Fig. 2 is only meant to convey the trend of the overall spectral change. Surprisingly, after a number of spectra with a peak position at ~ 810 nm, the emission spectrum returns to a wavelength close to the initial one at ~ 870 nm, albeit with the lower intensity (it is not clear what the implication is of this change since in the absence of the spectral changes the spectral intensity is generally rather constant). The most surprising finding is that in a remarkably large number of cases (50–90%) the intermediate FLP value of ~ 870 nm is regained after a period of 810 nm FL.

Comparison of the frequency of spectral jumping

A number of different criteria can be defined to assess the extent of spectral jumping of either individual complexes or populations of complexes from different species. In the latter case we pool the occurrences of spectral jumps from particular complexes to obtain the characteristics pertaining to a

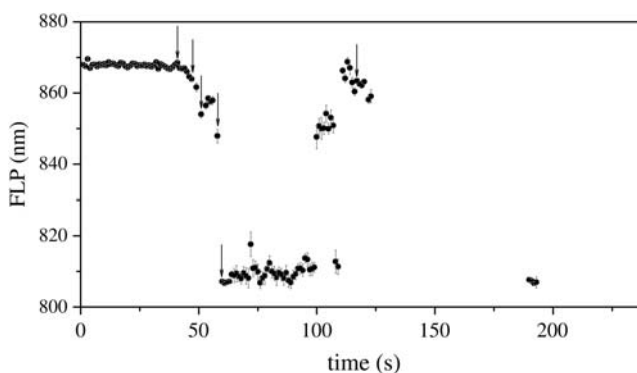


FIGURE 2 FLP trace of a single LH2 of *Rps. acidophila* with an extreme jump to ~ 810 nm. The arrowed spectra are depicted in Fig. 3.

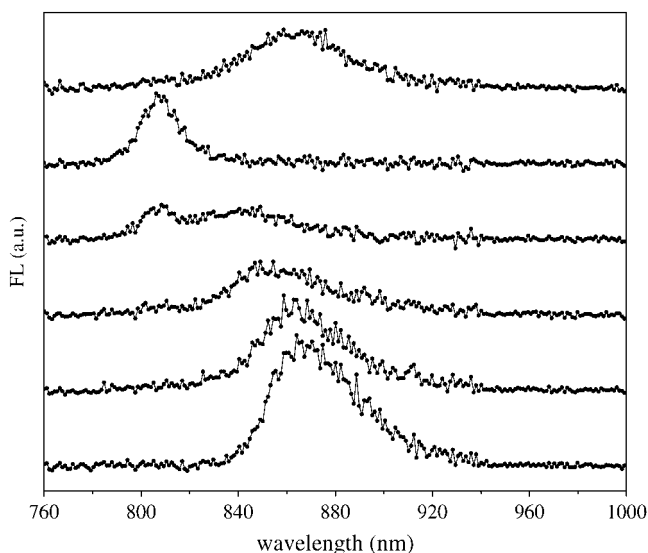


FIGURE 3 Selected spectra from Fig. 2: from bottom to top in increasing spectrum number.

species under certain experimental conditions. Examples of possible criteria are the distribution of standard deviation (STD) values of FLP time traces, distribution of FLP of all spectra from all particles constituting the experimental population, distribution of FLP differences between adjacent points in the time trace, and distribution of FLP differences relative to the beginning of the time trace. The first criterion allows for a comparison of the extent of spectral jumping between different experimental populations, but it does not convey the details of spectral jumping. The latter three are criteria that deal with changes in the FLP value between subsequent points in the FLP time trace. Thus they are sensitive to the immediate (with the limited time resolution of the experiment) but overlook overall spectral changes occurring over a few points in the time trace. The criterion we opt for in this work is the distribution of FLP changes using the sliding point definition. In this definition a spectral jump exceeding a certain threshold is recorded as follows: for the initial point of reference we take the first point in the time trace and search for the next point in the trace that deviates from the reference by more than a specified threshold. Once this happens, the jump is recorded, and the reference is transferred to the point where the jump occurred. This is repeated until the end of the trace for all the complexes (different time traces) in the population and for different threshold values. Such a procedure results in a distribution where each point indicates the number of jumps that are larger than the corresponding value of the threshold (Fig. 4). Although it does not provide the numbers of jumps of a specific size, the difference between two points in the histogram is the number of jumps of the size within the range set by the corresponding thresholds. In Fig. 4, at large values of the jump size the curves exhibit stretches of constant magnitude. That is because, due to the generally low

occurrence of large spectral changes, there are jump size intervals corresponding to zero occurrence.

These cumulative distributions are weighted with the total number of nonzero spectra in the experimental population and common multiplication factor equal to the average number of measured nonzero spectra. Such a normalization has to be done since different experimental populations contain unequal numbers of measured complexes with a varying percentage of nonzero spectra (note that spectral time traces consist of alternating emissive and dark periods).

One advantage of such a calculation in comparison with the other criteria is that it contains information about the overall spectral evolution (due to the definition of a jump by means of a “sliding point”) and at the same time it is sensitive to immediate spectral changes since a jump is also recorded in the cases when the difference between adjacent points in the trace is larger than a set threshold.

Since such a cumulative distribution does not directly convey information about the number of jumps of a certain size, we calculate the derivative of the distribution because it is equal to the number of jumps within a unit interval of the jump sizes. A comparison of the number of positive and negative jumps of different size occurring for all the different species with the same equivalent excitation intensity at 594 nm is shown in Fig. 5. The jump size scale upper limit is set to only 10 nm to emphasize the occurrence of jumps of intermediate magnitude, i.e., jumps that are larger than random spectral fluctuations and smaller than those with occurrence too small to make a sensible interspecies comparison. It appears from Fig. 5 that the general spectral jumping behavior of the different species is not strikingly divergent. The ratio between the most different occurrences of jumps of the same size for different species is not >3 . Moreover, the limited statistics of the data raise the question of how reliable and reproducible such differences are. To examine the reproducibility of such data, we have collected two data sets under identical experimental conditions for LH2 of *Rs. molischianum*. The difference between these data sets indicates the confidence margins of the frequency of spectral jumping for other species. It appears that the derivative curves of the positive and negative spectral jumps up to 5 nm can be separated in the ascending order: LH2 of *Rps. acidophila*, *Rb. sphaeroides*, and LH2 of *Rs. molischianum* and LH1 of *Rb. sphaeroides*. At jumps >5 nm, the relationship between the extents of the spectral changes for the different species becomes ambiguous due to the limited statistics of the available data.

Unfortunately we have to make this arbitrary separation between “intermediate” and “large” jumps at one value of the jump size of 5 nm due to the limited statistics of the jumps. Ideally we would extend the derivative dependence also into the range of large jumps of tens of nanometers. This would provide us with a means for a more detailed and specific distinction between the different species in terms of their conformational landscape that can be probed by

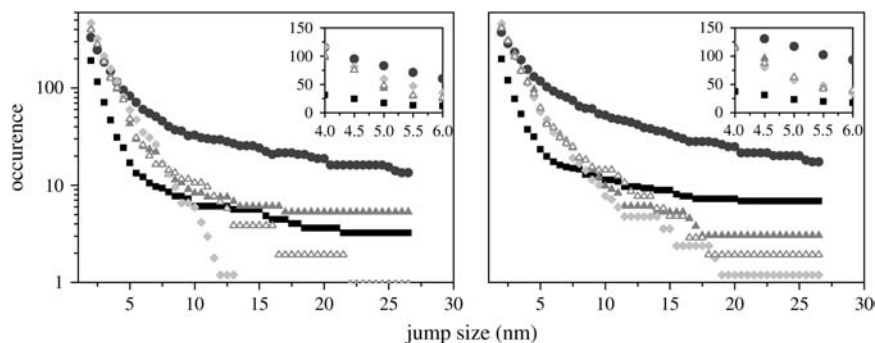


FIGURE 4 Cumulative histograms of positive (left panel) and negative (right panel) jumps with the sliding point definition for different species at 594 nm excitation. Plot legend is the same as in Fig. 5: LH2 of *Rps. acidophila*, solid squares; *Rb. sphaeroides*, dark shaded circles; *Rs. molischianum*, shaded full and open triangles; and LH1 of *Rb. sphaeroides*, light shaded diamonds. Insets magnify the area at ~ 5 nm jump size.

monitoring spectroscopic changes. We also recognize the fact that the distinction of large and intermediate spectral jumps with the threshold of 5 nm is highly arbitrary and is caused merely by statistical considerations. It has probably little or no relevance to the actual hierarchy of potential energy barriers in the conformational landscape of the pigment-proteins.

The numbers of positive and negative spectral jumps >5 nm in the case of LH2 of *Rps. acidophila* and *Rb. sphaeroides* also contain occurrences of extreme spectral jumping, since, as mentioned earlier, for these species FLP sometimes shifts to ~ 810 nm. Such dramatic changes occur neither for LH1 of *Rb. sphaeroides* nor for LH2 of *Rs. molischianum* (as mentioned earlier). Consequently, a comparison of frequencies of large spectral jumps (excluding extremities) for the different species should be done with somewhat lower values of jumps for the two species of LH2 of *Rps. acidophila* and *Rb. sphaeroides*. Taking this into account, this comparison is made from the cumulative distributions that at ~ 5 nm are shown as insets of the cumulative histograms in Fig. 4. In order of ascending number of positive and negative jumps >5 nm different complexes occur as LH2 of *Rps. acidophila*, LH2 of *Rs. molischianum* and LH1 of *Rb. sphaeroides*, and LH2 of *Rb. sphaeroides*.

The cumulative curves of LH1 of *Rb. sphaeroides* and LH2 of *Rps. acidophila* intersect at ~ 8 nm jump size indicating that the ratio of jumps >8 nm is reversed compared to that at 5 nm demanding a more detailed classification of the sizes of jumps at least for these two species.

However, the occurrence of jumps >8 nm is too scarce to conduct such detailed comparison.

Summarizing, LH2 of *Rps. acidophila* features the smallest number of both positive and negative spectral jumps of all sizes; LH2 of *Rs. molischianum* and LH1 of *Rb. sphaeroides* are similar to each other and exhibit the largest number of intermediate jumps and are in the second place for large jumps; LH2 of *Rb. sphaeroides* exhibits the biggest number of the large jumps and is in the second place for intermediate jumps.

Cumulative histograms and corresponding derivative curves resulting from an analogous measurement with 800 nm excitation for the different species are shown in Figs. 6 and 7, respectively. The derivative curves of the positive and negative jumps can be roughly divided into two groups: LH2 and LH1 of *Rb. sphaeroides* and the LH2 domain swap mutants jump more than LH2 of *Rps. acidophila* and *Rs. molischianum*. It is difficult to separate LH2 and LH1 of *Rb. sphaeroides* since the corresponding curves change their relative position both for positive and negative jumps even up to a jump size of 5 nm. The extent of positive spectral jumping of the two mutants of LH2 of *Rb. sphaeroides*, PACLH1 and PACLH2mol, is closer to the higher end of the observable jumping frequency for the different species, which is probably not too surprising, since the significant alteration of the native protein structure may be expected to destabilize these complexes. The corresponding negative jumps are less frequent in the data set probably due to the fact that the average spectrum of the mutants is strongly

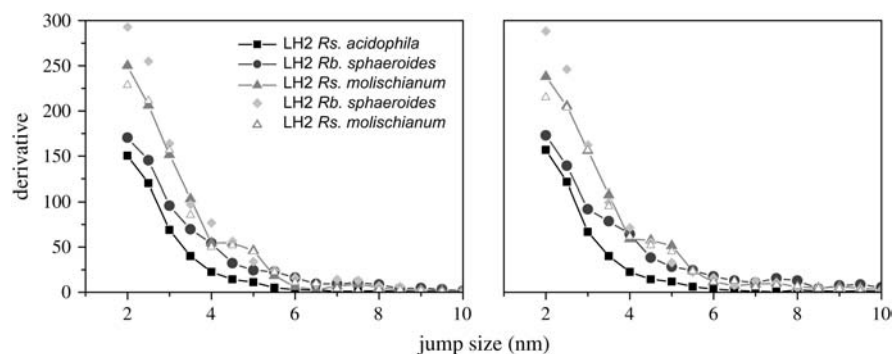


FIGURE 5 Derivatives of distributions of a number of jumps with the sliding point definition at 594 nm excitation. (Left panel) Positive jumps; (right panel) negative jumps.

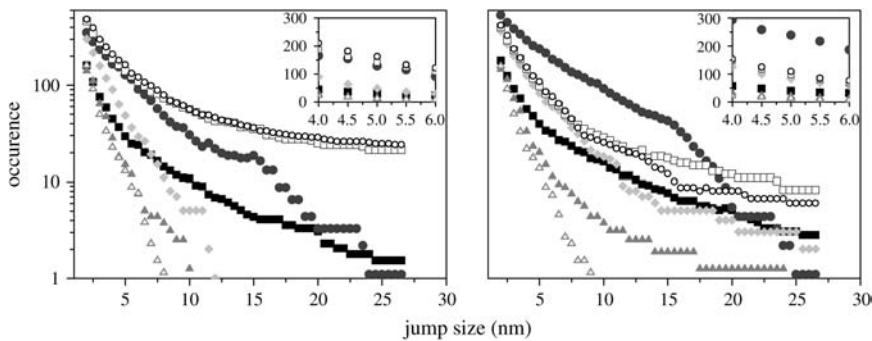


FIGURE 6 Cumulative histograms of positive (upper panel) and negative (lower panel) jumps with the sliding point definition for different species at 800 nm excitation. Plot legend is the same as in Fig. 7: LH2 of *Rps. acidophila*, solid squares; *Rb. sphaeroides*, dark shaded circles; *Rs. molischianum*, shaded full and open triangles; LH1 of *Rb. sphaeroides*, light shaded diamonds; PACLH1, open black squares; and PACLH2mol, open black circles. Insets magnify the area at ~ 5 nm jump size.

blue-shifted relative to the WT so that blue spectral occurrences are not visible due to the FL filter.

One distinct difference from the equivalent results with 594 nm excitation is that LH2 of *Rs. molischianum* has relatively few occurrences of jumps upon 800 nm excitation, and this result is reproducible for at least one more data set obtained under identical experimental conditions. A possible explanation of this apparent discrepancy is that we overestimate the number of absorbed photons upon 800 nm excitation, which is probably due to a partial bleaching of the B800 ring under intense excitation as this band was noticed to be more susceptible to biochemical and also illumination conditions (Dr. S. Georgakopoulou, Vrije Universiteit, personal communication, 2005). So in the following we will rely on the 594 nm excitation data set.

In terms of the large jumps upon 800 nm excitation, the various complexes are distributed in a similar manner as for 594 nm excitation with the exception of LH2 of *Rs. molischianum*—in ascending order of positive and negative jumps: LH2 of *Rps. acidophila*, LH1, and LH2 of *Rb. sphaeroides* (Fig. 6). The two mutants exhibit the largest occurrence not only of intermediate but also of large positive spectral jumps.

DISCUSSION

In this section, we summarize the occurrence of quasistable behavior and frequency of spectral jumping for different species and discuss the intriguing observation of the extreme blue spectral shifts. Then we investigate the microscopic origin of the interspecies variation of spectroscopic flexibility.

Extreme blue jumps

We observed that, in a number of cases, upon 594 nm excitation LH2 of *Rps. acidophila* and *Rb. sphaeroides* exhibited extreme blue spectral shifts down to FLP at ~ 810 nm, but this was not the case for the LH2 of *Rs. molischianum* or LH1 of *Rb. sphaeroides*. From the trace shown in Fig. 3 it appears that states with a moderately blue-shifted spectral peak wavelength serve as precursors for the final state with the FLP at ~ 810 nm (note that this does not imply that in all cases of spectral diffusion, each pigment-protein complex eventually arrives to this state). This spectral shift occurs through an intermediate spectrum that appears to be a superposition of spectral line shapes with the FLP value strongly blue-shifted relative to the intermediate one. It is unclear what the origin of this blue-shifted spectroscopic intermediate is, as it is not compatible with an intact B850 ring within the context of the proposed disordered exciton model. We propose that the emission spectrum peaking at 810 nm originates from the B800 ring in the absence of an efficient energy transfer to the B850 since it is twice as narrow as a typical spectrum at 870 nm and thus cannot originate from the exciton manifold of the B850 ring. The absence of B800-850 transfer step implies that the B850 is bleached, indicating extreme changes in the electronic structure of the ring that are probably associated with sizeable spatial rearrangement. It is rather surprising then that such a bleaching is reversible. The formation of an excitation trap in the B850 ring was used to explain the long nonradiative periods of LH2 of *Rps. acidophila* (38). This, however, cannot be used to explain our observations since, even in

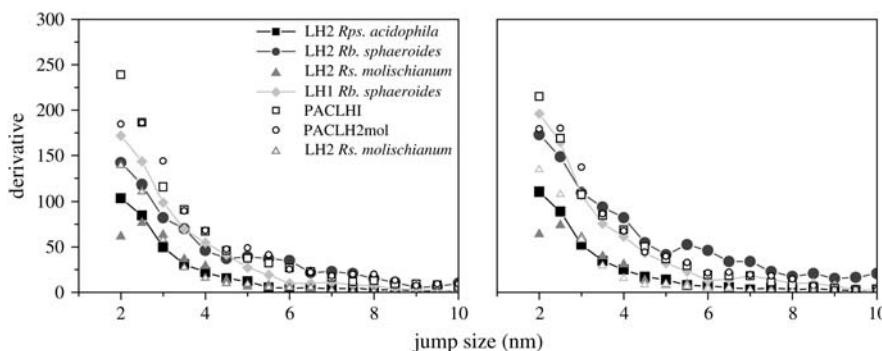


FIGURE 7 Derivatives of distributions of number of jumps with the sliding point definition at 800 nm excitation. (Left panel) Positive jumps; (right panel) negative jumps.

the presence of the trap, the B850 BChls *a* would still accept energy from the B800 BChls *a*. Thus these remarkable observations remain to be clarified in future investigations.

The above analysis demonstrates that in this experiment we exercise rather harsh excitation levels that can seriously destabilize the pigment-protein structure and in some cases to such an extent that, as we hypothesize above, one of the pigment rings is, at least temporarily, “spectroscopically” disabled. However, even if such a state is attained, it does not necessarily imply an irreparable damage of the pigment-protein, since in most cases the change appears to be reversible. This demonstrates the extreme robustness and flexibility of photosynthetic pigment-proteins allowing them to sustain activity even under excitation conditions that are remote from native and may represent an evolved stability to cope with abrupt large changes in illumination levels.

Quasistable FLP levels for different species

In terms of the occurrence and also of how distinctly different the observed quasistable states are, the different species are distributed in the following descending order: LH2 of *Rps. acidophila*, LH2 domain swap mutants of *Rb. sphaeroides*, LH2 of *Rb. sphaeroides*, LH1 of *Rb. sphaeroides* and LH2 of *Rs. molischianum*. It has to be noted that the quasistable states of the domain swap mutants occurred mostly with an FLP at ~880–890 nm, which indicates the existence of a well-defined stable conformation with this spectroscopic signature. In terms of an excitonic model, such red spectral shift can be associated with the red shifting of just one pigment in the B850 ring (V. Novoderezhkin, D. Rutkauskas, and R. van Grondelle, unpublished), which can be due to the strengthening of the H-bond to the acetyl group of the BChl *a* (see below) caused by structural deformation. Consequently, this state is probably associated with a local structural change of the proteic surroundings of one pigment. The LH2 domain swap mutants of *Rb. sphaeroides* have their C-terminal part of the α -polypeptide exchanged for corresponding sequences from the LH2 of *Rs. molischianum* or the LH1 of *Rb. sphaeroides* (34). These manipulations have altered the α Tyr+13 and α Tyr+14 residues, which in the native complex form H-bonds to the B850 BChls *a* and instead introduce only one candidate for H-bond formation, α Trp+11, which shifts the FL spectrum of the mutants to the blue. However, in that work the authors reported a red-shifted species as a minor component of the absorbance spectrum for both domain swap mutants. It is possible that these species reflected one of these long-lived quasistable states in vivo. The introduction of amino acids that are different to those in the LH2 WT structure appears to introduce conformational substates that are difficult to escape from, leading to the observed stable, strongly red-shifted, spectral states.

Our observations also allow us to approach the question of the hierarchical organization of the conformational land-

scape of the bacterial LHCs that was ascertained for the LH2 complex of *Rs. molischianum* in (21) following the proposed hierarchy of energy barriers for myoglobin (23). In the case where the energy barriers separating different conformations are organized in tiers according to their height, we should observe changes between spectroscopically different states associated with transitions over large energy barriers and smaller spectral fluctuations within those states corresponding to transitions over smaller barriers. In the case where the energy barriers are organized randomly, we should observe transitions between the different spectroscopic states perturbed only by the statistical fluctuations, alternating with smaller spectroscopic fluctuations associated with the crossing of smaller energy barriers. Our observation of the quasistable states indicates large energy barriers separating spectroscopically different states. We also observed fluctuations within those states. However, the spectral evolution also involves small spectral changes linking the large ones. Thus we can conclude that the actual conformational landscape of bacterial LHCs exhibits some hierarchical organization character, but with additional complexity that prevents its description purely in terms of the tier model of the energy barriers.

Comparison of the frequency of spectral jumping

A comparison of the frequency of spectral jumping for different species at two excitation wavelengths is made in Table 1. It appears that some observations are not reproduced between data sets with different excitation wavelengths. Thus, for example, we observed that the LH2 of *Rb. sphaeroides* with 594 nm excitation exhibits fewer intermediate and more large spectral jumps than the LH1 of *Rb. sphaeroides* or LH2 of *Rs. molischianum*. However in the data set at 800 nm excitation we could not make a distinction between the two groups in terms of intermediate jumps, and at the same time the relationship between the numbers of large jumps remained the same as in the 594 nm data set. We must conclude that the two species are similar in their frequency of intermediate jumps given the limited statistics of our data. Perhaps with better measurement statistics a distinction might be made.

From the combination of both data sets, we can make the following observations: for both positive and negative jumps of intermediate size, the LH2 of *Rps. acidophila* is spectroscopically the least flexible; the LH2 and LH1 of *Rb. sphaeroides* and the LH2 of *Rs. molischianum* exhibit similar levels of larger jumps. In terms of large positive and negative jumps the complexes are distributed in the following ascending order: LH2 of *Rps. acidophila*, LH1 of *Rb. sphaeroides* and LH2 of *Rs. molischianum*, and LH2 from *Rb. sphaeroides*. The two domain swap mutants feature the largest number of red jumps of all sizes. If we put more emphasis on the large spectral jumps then the corresponding list is LH2 of *Rps. acidophila*, LH2 of *Rs. molischianum* and LH1 of *Rb. sphaeroides*, and LH2 of *Rb. sphaeroides* in the order of increasing spectral flexibility.

TABLE 1 Experimental frequencies of positive and negative spectral jumps of intermediate and large size for different species

Frequency of spectral jumping	Intermediate jumps (594 nm)	Intermediate jumps (800 nm)	Large jumps (594 nm)	Large jumps (800 nm)
	LH2 <i>Rps. acidophila</i>	LH2 <i>Rs. molischianum</i> and <i>Rps. acidophila</i>	LH2 <i>Rps. acidophila</i>	LH2 <i>Rs. molischianum</i> LH2 <i>Rps. acidophila</i>
	LH2 <i>Rb. sphaeroides</i>	LH2 <i>Rb. sphaeroides</i> and LH1 <i>Rb. sphaeroides</i>	LH1 <i>Rb. sphaeroides</i> and LH2 <i>Rs. molischianum</i>	LH1 <i>Rb. sphaeroides</i>
	LH2 <i>Rs. molischianum</i> and LH1 <i>Rb. sphaeroides</i>		LH2 <i>Rb. sphaeroides</i>	LH2 <i>Rb. sphaeroides</i>
		Mutants (red jumps)		Mutants (red jumps)

The microscopic origin of spectral jumps

In this section we will discuss the microscopic parameters, determining the spectral properties of the B850 BChl *a* and structural flexibility of the complexes. We assume that structural changes induce alterations of those microscopic factors that are associated with the observed spectroscopic shifts. We further suggest that subtle differences in the chromophore binding pocket in different complexes determine their different spectroscopic response. In combination with differing structural flexibility this allows us to interpret the diversity of spectral flexibility among complexes.

The factors that have been considered as important in determining the pigment-protein electronic structure can be divided into two groups:

1. Pigment-pigment exciton coupling (13–19).
2. The tuning of the individual pigment site energy due to
 - a. Local protein environment:
 - i. point charges;
 - ii. H-bonding;
 - iii. axial ligation of Mg^{2+} .
 - b. Structural changes of the chromophore itself:
 - i. rotation of the C2 acetyl carbonyl group;
 - ii. distortion of porphyrin macrocycle (39–41).

The second set of factors determines the so-called pigment site energy, i.e., the electronic transition energy of the pigment in the absence of other pigments. Changes of these site energies are propagated by excitonic coupling over the delocalized electronic system of the ring of chromophores and are reflected in the absorption and FL properties.

Since the actual pigment site energy is a result of all the effects mentioned in 2, a comparison of the spectral properties of different species can only be made after a systematic analysis of the contribution of each parameter. Furthermore, the assessment of the relative spectral flexibility requires a detailed knowledge of the distance dependence of each factor and the trajectory of structural changes. In short, a complete model would require molecular dynamics simulations over long times that are not feasible at the moment and fall beyond the scope of this work. For this

reason, the effect of the above factors on the observed spectroscopic flexibility of the different species will only be assessed qualitatively.

To determine how each of the factors listed above influences the site energy and the spectroscopic properties of an individual pigment in a protein is a major problem in itself. Molecular orbital calculations indicate that placing point charges at 3.5 Å from rings A and C of a bacteriochlorin system produce Q_y absorption shifts in the order of 100 nm depending on the position and sign of the charge (30,31). And even in the case when such point charges are absent, the electric field emanating from the more distant parts of the surrounding protein must have an effect on the absorption (Stark effect). Formation of an H-bond to the acetyl group of BChl *a* has been calculated to red shift the absorption of Q_y by 6 nm, whereas an H-bond to the keto group causes a blue shift of the same magnitude (30). The latter are “pure” effects of H-bonding, i.e., they are due to the interaction of the ligand with the conjugated electronic system of the BChl *a* macrocycle. The rotation of the acetyl group out of the plane of the BChl *a* molecule causes a blue shift of the absorption of up to 20 nm for the Q_y transition, if the torsion angle assumes values of $\pm 90^\circ$ (29,30). The effect of a Mg^{2+} ligation is illustrated by the calculation of the exchange of the imidazole ligand (His) to a water molecule producing a blue shift of the Q_y absorption of 3 nm (30). Calculations suggest that distortions of the porphyrin macrocycle may lead to the absorption red shifts in the order of 100 nm in extreme cases (42). All of these contributions to BChl red shifts were discussed extensively in Gall et al. (43).

From the comparison of the above numbers it appears that point charges, the rotation of the acetyl group, and the deformation of the porphyrin ring have the largest spectroscopic impact. In the B850 ring of the complexes investigated there are no point charges in the proximity of the BChl *a* macrocycles. The macrocycle of at least one of the B850 BChl *a* molecules is strongly distorted in a number of different LHCs (44), and the acetyl carbonyl group is rotated out of the molecular plane (41).

Deformation of the porphyrin ring is thought to be due to the H-bonding of its peripheral groups and ligation of the

central Mg^{2+} ion (45). H-bonding also determines the position of the acetyl carbonyl group relative to the molecular plane (41). The structural configuration of the pigment must also be influenced by mechanical effects such as van der Waals interactions within the pigment-protein. However, accounting for such an effect can only be done by molecular dynamics simulations and will not be considered here.

Thus we have narrowed down the list of all the microscopic factors to those which are spectroscopically most significant: the porphyrin macrocycle deformation and the acetyl group rotation, which are at least partly accounted for by the H-bonding to the acetyl carbonyl. Furthermore, systematic mutational studies have revealed a linear relationship between the H-bonding strength to the acetyl carbonyls of the B850 BChls *a* and the absorption peak wavelength (46,47). This allows us to correlate the observable spectroscopic jumps to structural changes by means of the changes in the H-bonding strength. The weakening of the H-bond to the acetyl carbonyl allows its rotation further out of the molecular plane (41) and probably relaxes the deformation of the porphyrin ring, which together leads to a blue spectral shift, whereas the strengthening of the bond has an opposite effect, causing a red shift. This way the observed blue and red spectral shifts can be interpreted.

The relative structural flexibility of different species is assessed based on the network of H-bonds described above. In the LH2 of *Rps. acidophila* and *Rb. sphaeroides*, the α -polypeptide donates one H-bond to the acetyl carbonyl of BChl *a* in the same dimeric subunit and a second one to the BChl *a* in the adjacent subunit; H-bonds between different subunits contribute to the structural stabilization of the complex as a whole. However, in LH2 of *Rs. molischianum* and LH1 of *Rb. sphaeroides*, the H-bonds to the acetyl carbonyl as well as to the keto groups of the BChls *a* are internal to the subunit. This difference in the H-bonding pattern is proposed to be associated with the different structural flexibility of the LH2 of *Rb. sphaeroides* and the LH1 of *Rb. sphaeroides*: the former is considered to be less flexible than the latter (48). In addition to this, LH1 is thought to be more flexible partly due to its larger size.

The acetyl carbonyl H-bonding strength is experimentally assessed by the downshift of a corresponding spectral Raman peak (which in the absence of H-bonding is $\sim 1660\text{ cm}^{-1}$); together with proposed structural flexibilities these strengths for different species are summarized in Table 2.

In the following, we interpret the intercomplex variation of spectroscopic flexibility based on differences in the struc-

tural flexibility and the H-bonding strength. The possible structural changes are presumed to be associated with changes in the H-bonding strength. It is assumed that the stronger the H-bond, the larger its change may be in response to structural alteration. Since the spectral change and that of the H-bonding strength are proportional, the former is also larger in the case where a strong H-bond is perturbed. Thus, for example, LH1 of *Rb. sphaeroides* and LH2 of *Rs. molischianum* are structurally flexible, but their H-bonding to the acetyl carbonyl is associated with only an 18 cm^{-1} downshift of the corresponding Raman peak. This implies frequent structural changes with little spectroscopic consequence, which results in a similar intermediate spectroscopic flexibility of the two complexes as was observed experimentally. The absence of stable conformations complies with the observed absence of quasistable FLP states.

The LH2 of *Rb. sphaeroides* is less flexible but its H-bonding corresponds on the average to a downshift of the Raman peak of $\sim 29\text{ cm}^{-1}$. Consequently, structural changes, although less frequent, will result in larger spectroscopic alterations, leading to a large observed spectral flexibility. Intermediate occurrence of quasistability is associated with some conformations from which it is difficult to escape.

Finally, LH2 of *Rps. acidophila* exhibits H-bonding as strong as that of *Rb. sphaeroides*, which means that the same structural changes will be associated with similar spectral alterations for both complexes. However, the spectroscopic flexibility of LH2 of *Rps. acidophila* is observed to be the lowest of all complexes investigated. Since there is no quantitative criterion of structural flexibility, it might be that although both LH2 of *Rps. acidophila* and *Rb. sphaeroides* are rather structurally rigid the former is more inflexible than the latter due to other differences in their protein backbones, resulting in fewer structural changes, which leads to a lower spectral flexibility. This also implies that the LH2 of *Rps. acidophila* must exhibit more stable conformations, which is corroborated by the observed multitude of quasistable states of FLP.

Although rather qualitative, the above speculations allow us to interpret the observed differences in spectroscopic flexibility among the various complexes. This analysis is instructive as it shows that structural flexibility, although related, is not identical to the experimentally observable frequency of spectral jumping. For example, LH1 is supposed to be more flexible than any of the LH2 complexes due to its larger size; however, its spectral flexibility is of an intermediate magnitude probably due to the weaker connection between structural and spectroscopic changes. Thus, when considering flexibilities one should be careful as to exactly which issue is addressed.

TABLE 2 Strength of H-bonding to carbonyl acetyls of B850 BChls *a* and structural flexibility of different complexes

Species	Acetyl downshift (cm^{-1})	Reference	Flexible
LH2 <i>Rps. acidophila</i>	30 (degenerate)	(49)	No
LH2 <i>Rb. sphaeroides</i>	32 and 25	(27)	No
LH2 <i>Rs. molischianum</i>	18 (degenerate)	(50)	Yes
LH1 <i>Rb. sphaeroides</i>	18 (degenerate)	(35)	Yes

CONCLUSIONS

In this work, we have conducted a comparative study of FL spectral evolution of different kinds of single bacterial

LHCs. We previously observed that the FLP of single LH2 of *Rps. acidophila* evolved through different quasistable states. Here we found that to various extents this is a property of other types of bacterial LHCs.

Moreover, an improved experimental arrangement allowed the observation of extreme spectral jumps to the blue that we associated with bleaching of one of the pigment rings, which is probably connected to a sizable structural rearrangement. It is surprising that such transitions are often reversible implying the recovery of the destabilized ring.

The measurement of FL spectral traces of a number of individual complexes allowed us to build the statistics of spectral jumping. The investigated pigment-proteins are rather complex systems, and an unambiguous connection between the experimentally observable FL spectral change and corresponding structural deformation cannot be made at the moment. However, we conclude that the observed variation of frequency and size of spectral jumping of different LHCs must be associated with different structural flexibilities of the pigment-proteins and a variation of the strength of the factors determining the electronic transition (site) energies of the chromophores.

We thank Dr. E. Papagiannakis for critically reviewing the manuscript.

This research was supported by the Netherlands Organization for Scientific Research. J. Olsen, C. N. Hunter, A. Gall, and R. J. Cogdell gratefully acknowledge the support of the Biotechnology and Biological Sciences Research Council UK.

REFERENCES

- van Grondelle, R., J. P. Dekker, T. Gillbro, and V. Sundström. 1994. Energy-transfer and trapping in photosynthesis. *Biochim. Biophys. Acta*. 1187:1–65.
- Koepke, J., X. C. Hu, C. Muenke, K. Schulten, and H. Michel. 1996. The crystal structure of the light-harvesting complex II (B800–850) from *Rhodospirillum rubrum*. *Structure*. 4:581–597.
- McDermott, G., S. M. Prince, A. A. Freer, A. M. Hawthornthwaite, M. Z. Papiz, R. J. Cogdell, and N. W. Isaacs. 1995. Crystal structure of an integral membrane light-harvesting complex from photosynthetic bacteria. *Nature*. 374:517–521.
- Papiz, M. Z., S. M. Prince, T. Howard, R. J. Cogdell, and N. W. Isaacs. 2003. The structure and thermal motion of the B800–850 LH2 complex from *Rps. acidophila* at 2.0 Å resolution and 100 K: new structural features and functionally relevant motions. *J. Mol. Biol.* 326:1523–1538.
- Cogdell, R. J., P. K. Fyfe, S. J. Barrett, S. M. Prince, A. A. Freer, N. W. Isaacs, P. McGlynn, and C. N. Hunter. 1996. The purple bacterial photosynthetic unit. *Photosynth. Res.* 48:55–63.
- Hu, X. C., T. Ritz, A. Damjanovic, F. Autenrieth, and K. Schulten. 2002. Photosynthetic apparatus of purple bacteria. *Q. Rev. Biophys.* 35:1–62.
- Robert, B., R. J. Cogdell, and R. van Grondelle. 2003. The light-harvesting system of purple bacteria. In *Light-Harvesting Antennas in Photosynthesis*. B. R. Green and W. W. Parson, editors. Kluwer Academic Publishers, Dordrecht, The Netherlands. 169–194.
- Sundström, V., T. Pullerits, and R. van Grondelle. 1999. Photosynthetic light-harvesting: reconciling dynamics and structure of purple bacterial LH2 reveals function of photosynthetic unit. *J. Phys. Chem. B*. 103:2327–2346.
- Fotiadis, D., P. Qian, A. Philippsen, P. A. Bullough, A. Engel, and C. N. Hunter. 2004. Structural analysis of the reaction center light-harvesting complex I photosynthetic core complex of *Rhodospirillum rubrum* using atomic force microscopy. *J. Biol. Chem.* 279:2063–2068.
- Conroy, M. J., W. H. J. Westerhuis, P. S. Parkes-Loach, P. A. Loach, C. N. Hunter, and M. P. Williamson. 2000. The solution structure of *Rhodobacter sphaeroides* LH1 beta reveals two helical domains separated by a more flexible region: structural consequences for the LH1 complex. *J. Mol. Biol.* 298:83–94.
- Karrasch, S., P. A. Bullough, and R. Ghosh. 1995. The 8.5 Å projection map of the light-harvesting complex-I from *Rhodospirillum rubrum* reveals a ring composed of 16 subunits. *EMBO J.* 14:631–638.
- Walz, T., S. J. Jamieson, C. M. Bowers, P. A. Bullough, and C. N. Hunter. 1998. Projection structures of three photosynthetic complexes from *Rhodobacter sphaeroides*: LH2 at 6 Å LH1 and RC-LH1 at 25 Å. *J. Mol. Biol.* 282:833–845.
- Alden, R. G., E. Johnson, V. Nagarajan, W. W. Parson, C. J. Law, and R. J. Cogdell. 1997. Calculations of spectroscopic properties of the LH2 bacteriochlorophyll-protein antenna complex from *Rhodospseudomonas acidophila*. *J. Phys. Chem. B*. 101:4667–4680.
- Hu, X. C., T. Ritz, A. Damjanovic, and K. Schulten. 1997. Pigment organization and transfer of electronic excitation in the photosynthetic unit of purple bacteria. *J. Phys. Chem. B*. 101:3854–3871.
- Novoderezhkin, V., R. Monshouwer, and R. van Grondelle. 1999. Exciton (de)localization in the LH2 antenna of *Rhodobacter sphaeroides* as revealed by relative difference absorption measurements of the LH2 antenna and the B820 subunit. *J. Phys. Chem. B*. 103:10540–10548.
- Novoderezhkin, V., M. Wendling, and R. van Grondelle. 2003. Intra- and interband transfers in the B800–B850 antenna of *Rhodospirillum rubrum*: redfield theory modeling of polarized pump-probe kinetics. *J. Phys. Chem. B*. 107:11534–11548.
- Scholes, G. D., and G. R. Fleming. 2000. On the mechanism of light harvesting in photosynthetic purple bacteria: B800 to B850 energy transfer. *J. Phys. Chem. B*. 104:1854–1868.
- van Grondelle, R., and V. Novoderezhkin. 2001. Dynamics of excitation energy transfer in the LH1 and LH2 light-harvesting complexes of photosynthetic bacteria. *Biochemistry*. 40:15057–15068.
- Wu, H. M., M. Rätsep, I. J. Lee, R. J. Cogdell, and G. J. Small. 1997. Exciton level structure and energy disorder of the B850 ring and the LH2 antenna complex. *J. Phys. Chem. B*. 101:7654–7663.
- van Oijen, A. M., M. Ketelaars, J. Köhler, T. J. Aartsma, and J. Schmidt. 2000. Spectroscopy of individual light-harvesting 2 complexes of *Rhodospseudomonas acidophila*: diagonal disorder, inter-complex heterogeneity, spectral diffusion, and energy transfer in the B800 band. *Biophys. J.* 78:1570–1577.
- Hofmann, C., T. J. Aartsma, H. Michel, and J. Köhler. 2003. Direct observation of tiers in the energy landscape of a chromoprotein: a single-molecule study. *Proc. Natl. Acad. Sci. USA*. 100:15534–15538.
- Rutkauskas, D., V. Novoderezhkin, R. J. Cogdell, and R. van Grondelle. 2004. Fluorescence spectral fluctuations of single LH2 complexes from *Rhodospseudomonas acidophila* strain 10050. *Biochemistry*. 43:4431–4438.
- Frauenfelder, H., P. J. Steinbach, and R. D. Young. 1989. Conformational relaxation in proteins. *Chem. Scr.* 29A:145–150.
- Cogdell, R. J., T. D. Howard, N. W. Isaacs, K. McLuskey, and A. T. Gardiner. 2002. Structural factors which control the position of the Q_y absorption band of bacteriochlorophyll a in purple bacterial antenna complexes. *Photosynth. Res.* 74:135–141.
- Zuber, H., and R. A. Brunisholz. 1991. Structure and function of antenna polypeptides and chlorophyll-protein complexes: principles and variability. In *Chlorophylls*. H. Sheer, editor. CRC, Boca Raton, FL. 627–703.
- Fowler, G. J. S., G. D. Sockalingum, B. Robert, and C. N. Hunter. 1994. Blue shifts in bacteriochlorophyll absorbance correlate with changed hydrogen-bonding patterns in light-harvesting LH2 mutants of *Rhodobacter sphaeroides* with alterations at αTyr44 and αTyr45. *Biochem. J.* 299:695–700.

27. Fowler, G. J. S., R. W. Visschers, G. G. Grief, R. van Grondelle, and C. N. Hunter. 1992. Genetically modified photosynthetic antenna complexes with blueshifted absorbency bands. *Nature*. 355:848–850.
28. Hu, X., and K. Schulten. 1998. Model for the light-harvesting complex I (B875) of *Rhodobacter sphaeroides*. *Biophys. J.* 75:683–694.
29. Gudowskanowak, E., M. D. Newton, and J. Fajer. 1990. Conformational and environmental effects on bacteriochlorophyll optical spectra—correlations of calculated spectra with structural results. *J. Phys. Chem.* 94:5795–5801.
30. Hanson, L. K., M. A. Thompson, and J. Fajer. 1987. Environmental effect of properties of chlorophylls in vivo. Theoretical models. In *Progress in Photosynthesis Research*. J. Biggins, editor. Martinus Nijhoff, Dordrecht, The Netherlands. 311–314.
31. Eccles, J., and B. Honig. 1983. Charged amino-acids as spectroscopic determinants for chlorophyll in vivo. *Proc. Natl. Acad. Sci. USA*. 80: 4959–4962.
32. Pfenning, N. 1969. *Rhodospseudomonas acidophila*, a new species of the budding purple non-sulfur bacteria. *J. Bacteriol.* 99:597–602.
33. Evans, M. B., A. M. Hawthornthwaite, and R. J. Cogdell. 1990. Isolation and characterisation of the different B800–850 light-harvesting complexes from low- and high-light grown cells of *Rhodospseudomonas palustris*, strain 2.1.6. *Biochim. Biophys. Acta*. 1016:71–76.
34. Olsen, J. D., B. Robert, A. Siebert, P. A. Bullough, and C. N. Hunter. 2003. Role of the C-terminal extrinsic region of the alpha polypeptide of the light-harvesting 2 complex of *Rhodobacter sphaeroides*: a domain swap study. *Biochemistry*. 42:15114–15123.
35. Olsen, J. D., G. D. Sockalingum, B. Robert, and C. N. Hunter. 1994. Modification of a hydrogen bond to a bacteriochlorophyll a molecule in the light-harvesting 1 antenna of *Rhodobacter sphaeroides*. *Proc. Natl. Acad. Sci. USA*. 91:7124–7128.
36. Rutkauskas, D., V. Novoderezhkin, R. J. Cogdell, and R. van Grondelle. 2005. Fluorescence spectroscopy of conformational changes of single LH2 complexes. *Biophys. J.* 88:422–435.
37. Sturgis, J. N., C. N. Hunter, and R. A. Niederman. 1988. Spectra and extinction coefficients of near infrared absorption bands in membranes of *Rhodobacter sphaeroides* mutants lacking light-harvesting and reaction center complexes. *Photochem. Photobiol.* 48:243–247.
38. Bopp, M. A., Y. W. Jia, L. Q. Li, R. J. Cogdell, and R. M. Hochstrasser. 1997. Fluorescence and photobleaching dynamics of single light-harvesting complexes. *Proc. Natl. Acad. Sci. USA*. 94:10630–10635.
39. Cogdell, R. J., N. W. Isaacs, A. A. Freer, J. Arrelano, T. D. Howard, M. Z. Papiz, A. M. Hawthornthwaite, and S. Prince. 1997. The structure and function of the LH2 (B800–850) complex from the purple photosynthetic bacterium *Rhodospseudomonas acidophila* strain 10050. *Prog. Biophys. Mol. Biol.* 68:1–27.
40. He, Z., V. Sundström, and T. Pullerits. 2002. Influence of the protein binding site on the excited states of bacteriochlorophyll: DFT calculations of B800 in LH2. *J. Phys. Chem. B*. 106:11606–11612.
41. McLuskey, K., S. M. Prince, R. J. Cogdell, and N. W. Isaacs. 2001. The crystallographic structure of the B800–820 LH3 light-harvesting complex from the purple bacteria *Rhodospseudomonas acidophila* strain 7050. *Biochemistry*. 40:8783–8789.
42. Barkigia, K. M., L. Chantranupong, K. M. Smith, and J. Fajer. 1988. Structural and theoretical models of photosynthetic chromophores—implications for redox, light-absorption properties and vectorial electron flow. *J. Am. Chem. Soc.* 110:7566–7567.
43. Gall, A., J. D. Sturgis, G. J. S. Fowler, C. N. Hunter, and B. Robert. 1997. Influence of the protein binding site on the absorption properties of the monomeric bacteriochlorophyll in *Rhodobacter sphaeroides* LH2 complex. *Biochemistry*. 36:16282–16287.
44. Lapouge, K., A. Naveke, A. Gall, A. Ivancich, J. Seguin, H. Scheer, J. N. Sturgis, T. A. Mattioli, and B. Robert. 1999. Conformation of bacteriochlorophyll molecules in photosynthetic proteins from purple bacteria. *Biochemistry*. 38:11115–11121.
45. Scheidt, W. R., and Y. J. Lee. 1987. Recent advances in the stereochemistry of metallochlorophylls. In *Structure and Bonding*. J. W. Buchler, editor. Springer-Verlag, Berlin. 1–70.
46. Sturgis, J. N., J. D. Olsen, B. Robert, and C. N. Hunter. 1997. Functions of conserved tryptophan residues of the core light-harvesting complex of *Rhodobacter sphaeroides*. *Biochemistry*. 36:2772–2778.
47. Sturgis, J. N., and B. Robert. 1997. Pigment binding-site and electronic properties in light-harvesting proteins of purple bacteria. *J. Phys. Chem. B*. 101:7227–7231.
48. Bahatyrova, S., R. N. Frese, K. O. van der Werf, C. Otto, C. N. Hunter, and J. D. Olsen. 2004. Flexibility and size heterogeneity of the LH1 light harvesting complex revealed by atomic force microscopy—functional significance for bacterial photosynthesis. *J. Biol. Chem.* 279: 21327–21333.
49. Robert, B., A. Vermeglio, R. Steiner, H. Scheer, and M. Lutz. 1988. In *Photosynthetic Light Harvesting Systems: Organizations and Functions: Proceedings*. H. Scheer and S. Schneider, editors. De Gruyter & Co., Berlin and New York. 355–363.
50. Germeroth, L., F. Lottspeich, B. Robert, and H. Michel. 1993. Unexpected similarities of the B800–850 light-harvesting complex from *Rhodospirillum rubrum* to the B870 light-harvesting complexes from other purple photosynthetic bacteria. *Biochemistry*. 32: 5615–5621.